Optical Suppression of Photoassociative Ionization in a Magneto-Optical Trap

L. Marcassa, S. Muniz, E. de Queiroz, S. Zilio, and V. Bagnato
Instituto de Física e Química de São Carlos, University of São Paulo São Carlos, São Paulo 13560, Brazil

J. Weiner
Department of Chemistry and Biochemistry, University of Maryland, College Park, Maryland 20742

P. S. Julienne
Molecular Physics Division, National Institute of Standards and Technology, Gaithersburg, Maryland 20899

K.-A. Suominen
Clarendon Laboratory, Department of Physics, University of Oxford, Parks Road, Oxford OX13PU, United Kingdom
(Received 28 January 1994)

We demonstrate suppression of two-color photoassociative ionization in a sodium vapor magneto-optical trap by imposing an auxiliary "suppressor" light beam on the ensemble of colliding trapped atoms. We interpret the experimental results in terms of a simple picture in which the suppressor light intercepts incoming reactant particle flux and reroutes it to long-range repulsive states, effectively preventing further approach of the collision pairs.

PACS numbers: 32.80.Pj, 33.80.Ps, 34.50.Rk, 34.80.Qb

The ultracold environment produced by a magneto-optic trap (MOT) is a convenient reaction vessel in which to study two-body inelastic collision processes [1]. Although the study of collisional trap loss [2–4] has played a major role in revealing the nature of the ultracold regime, to date, only photoassociative ionization (PAI) [1] has permitted direct measure of the reaction product as a function of various probe fields and trap parameters. Previous studies demonstrated that one- or two-color light fields initiate PAI by a two-step process [5,6]. In the first step, incoming ground-state reactant atom pairs absorb a photon to excited *attractive* states at very long range. Subsequent acceleration on the $-C_3/R^3$ attractive potential to shorter range together with absorption of a second photon (of the same or different color) to a doubly excited state leads to the final collision product.

Here we report an experiment in which the normal PAI process is interrupted at the first step by switching the initial colliding pair to *repulsive* $+C_3/R^3$ states at long range, thereby preventing the atoms from entering the inner zone in which the second transition to the doubly excited state can take place. Previous experiments have demonstrated that light fields can be used to open or amplify inelastic channels. This experiment demonstrates that light fields can suppress inelastic processes as well. Optical suppression may prove useful in overcoming some collisional heating processes that presently limit the density of ultracold atomic ensembles [1,7].

The experimental setup is similar to the one described in an earlier report [6]. Figure 1 schematically outlines the arrangement. Sodium vapor at a partial pressure corresponding to ~80 °C, contained in a chamber at a base pressure lower than 10^{-6} Pa (10^{-8} Torr), provides the atoms that load a MOT. The trap is formed by three mutually orthogonal laser beams intersecting at the center of a quadrupole magnetic field, generated by a pair of coils carrying opposite currents. The coils are located external to the chamber and produce a field gradient in the trap region 0.2 $\mathrm{T\,m^{-1}}$ (20 $\mathrm{G\,cm^{-1}}$). An Ar^+ ion-pumped dye laser (laser 1) provides the light for the trap beams and the PAI suppressor beam. The 700 mW total output power of laser 1 splits into two beams. Beam 1 (~500 mW) is used to produce the MOT itself; it passes through an electro-optic modulator (EOM 1) that introduces sidebands at 1712 MHz to the red and blue of the central frequency. Modulation efficiency of EOM 1 is such that total power is equally divided

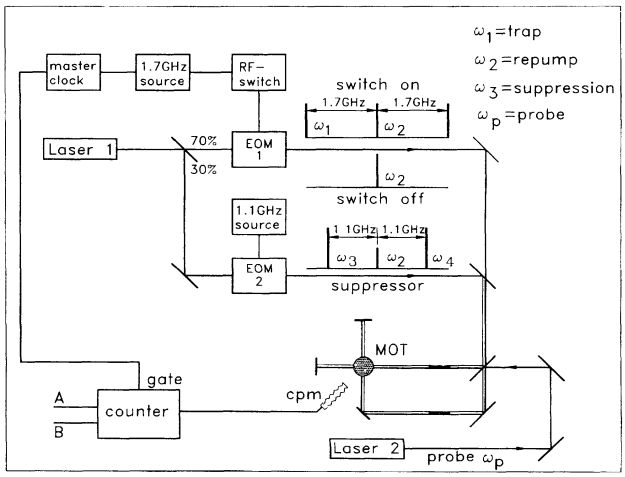

FIG. 1. Schematic diagram of the apparatus. The sidebands and carrier on the MOT laser are separated by 1712 MHz. The sidebands and carrier on the suppressor laser are separated by 1120 MHz.

between carrier and sidebands. The carrier is tuned to the repumper transition $[3\,^2S_{1/2}(F = 1) \rightarrow 3\,^2P_{3/2}(F' = 2)]$ frequency ω_2, while the red sideband ω_1 excites the cooling transition $[3\,^2S_{1/2}(F = 2) \rightarrow 3\,^2P_{3/2}(F' = 3)]$.

Beam 2 (~200 mW) passes through a second modulator (EOM 2), producing red and blue sidebands (ω_3, ω_4, respectively) 1120 MHz on each side of the ω_2 carrier. The red sideband ω_3 functions as the suppressor beam. We carried out two separate experiments: one with power in each of the ω_3, ω_4 sidebands of about 70 mW and the other with the power increased in each of the sidebands by a factor of 3.

Measurement of the laser beam diameter ($1/e^2$ points) determined the power density of the suppressor beam at the position of the MOT to be 0.4 and 1.2 $\mathrm{W\,cm^{-2}}$, respectively. The rf radiation exciting EOM 1 passes through a fast switch to modulate the appearance of the sidebands in beam 1. Focusing optics, external to the MOT chamber, capture a fraction of the trap fluorescence and image it onto a photodiode. The fluorescence monitors the number of atoms in the trap to ensure stability as the experiment is carried out.

A second ring laser (laser 2), with a total output power of about 30 mW, provides the scanning probe beam ω_p. While the probe beam scans over a range of about 4 GHz, ions (Na_2^+) produced in the trap are collected by a channeltron particle multiplier (CPM) mounted about 28 mm from the trap. A two-channel gated counter registers the charge pulses generated at the CPM after filtering through a fast amplifier discriminator. A master clock synchronizes switching of the MOT sideband modulation and counter gates for channel A (sidebands off) and channel B (sidebands on). Details of the switching and gating are described elsewhere [6].

As the probe laser frequency ω_p scans, we measure the ion spectrum at channel A (sidebands off) with the suppressor beam either switched off or on. Optical pumping transfers virtually all population to the $F = 2$ ground level within the 10 μs delay between switching off the sidebands and gating on the A channel. Therefore the incoming scattering flux always starts on the $F = 2 + F = 2$ ground-state molecular asymptote (see Figs. 3(b), 3(c), and 3(d).

Figure 2 (solid line) shows the ion spectrum versus $(\omega_p - \omega_1)/2\pi$ detuning with the suppressor beam switched off. The ~350 MHz "hole" centered on the zero of detuning is due to severe disturbance of the trap by the probe laser. As the probe laser scans to lower frequency, we observe structured features with intensity degrading to the red, identical to those reported previously [6]. This structure is believed to be due to long-range free-bound vibronic transitions from the ground-state continuum to bound levels of the 0_g^- "bundle" of hyperfine states correlating to the $^2P_{3/2} + {}^2S_{1/2}(F = 2)$ asymptote.

The path of the scattering flux, or quantum mechanical current J, leading to the final Na_2^+ ion product

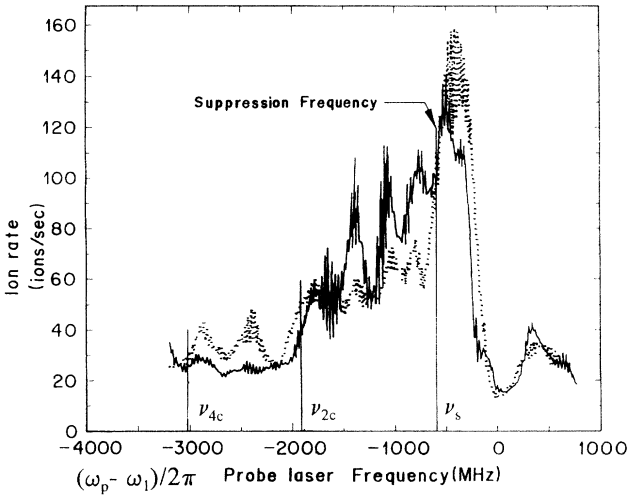

FIG. 2. The solid line is the normal two-color photoassociative ionization spectrum without the suppressor beam. The dotted line shows the same spectral region with the suppressor beam (0.4 $\mathrm{W\,cm^{-2}}$) applied to the MOT. As ω_p scans to the red, note that the detuning point ν_S at which the intensity switches from enhanced to suppressed is $\nu_S = \omega_S/2\pi = -(\omega_3 - \omega_1)/2\pi = -592$ MHz. Note also that the red detuning cutoff ν_{2c} for TCPAI, due to the presence of carrier frequency ω_2, is $(\omega_2 - \omega_1)/2\pi - 210$ MHz $= -1922$ MHz, and the red detuning cutoff for TCPAI, due to the presence of frequency ω_4, is $\nu_{4c} = -(\omega_4 - \omega_1)/2\pi - 210$ MHz $= -3042$ MHz. The 210 MHz term in ν_{2c} and ν_{4c} comes from coupling to the lowest lying level $[3p(F = 0) + 3p(F = 0)]$ of the doubly excited state.

is sketched in Fig. 3(b). Atom pairs on the 2 + 2 ground-state potential (curve A) approach each other with unit flux, absorbing a photon ω_p from the probe laser and undergoing a transition to the bound levels of the attractive $-C_3/R^3$ potential (curve B). The transition occurs in a localized region around the Condon point R_p, where $\hbar\omega_p$ matches the difference between the two potential curves A and B. The atom pair accelerates along curve B until it reaches a second Condon point R_2, where $\hbar\omega_2$ matches the difference between curves B and D. Absorption around this second Condon point promotes the collision pair to the doubly excited level (curve D). The bound-state vibrational motion on curve B produces multiple passes through this crossing [8].

Finally, after entering the inner zone of internuclear distance where the doubly excited level becomes degenerate with the ion molecule, the collision pair autoionizes to produce Na_2^+. Figure 2 (dotted line) traces the spectrum with the suppressor sideband ω_3 (and ω_4) switched on. The suppressor light alters the usual spectral features in three ways: (1) When the probe frequency scans to the red side of $\omega_S = -(\omega_3 - \omega_1)/2\pi = -592$ MHz, the ion intensity is suppressed by about 30%; (2) when the probe scans to the blue of ω_S, the intensity is enhanced by about the same fraction; and (3) the base line near the red limit

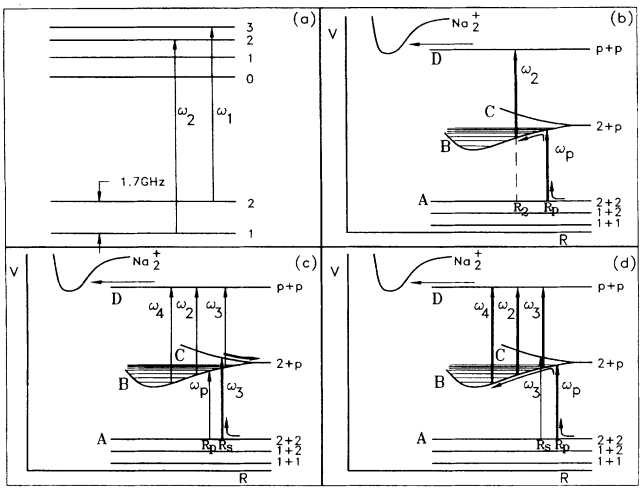

FIG. 3. (a) Relation between trap frequency ω_1 and repumper frequency ω_2. (b) Probe frequency ω_p scanning to the red of ω_3. The normal pathway is suppressed by $\hbar\omega_3$ coupling of the 2 + 2 ground state to the 2 + p repulsive level. (c) Probe frequency ω_p scanning to the blue of ω_3. The normal pathway is enhanced by $\hbar\omega_3$ coupling of the 2 + p attractive level to the p + p doubly excited level.

of the scan continues to show small but measurable intensity together with vibrational features. We interpret this modified spectrum in terms of the potential curves and transitions sketched in Figs. 3(c) and 3(d).

Figure 3(c) shows that when ω_p is tuned to the red of ω_3, the normal route to PAI is interrupted by the suppressor frequency which couples the incoming reactant flux from the flat ground-state potential (curve A) to the $+C_3/R^3$ repulsive curve (curve C) around the Condon point R_S. This transfer of scattering flux to a repulsive level prevents the collision pair from approaching the autoionization zone and effectively quenches PAI. However, as shown in Figs. 3(c–d), ω_3 also couples the attractive $-C_3/R^3$ curve (curve B) to the doubly excited level (curve D) at R_S. Therefore, when ω_p scans to the blue side of ω_3, this coupling *enhances* PAI, because now both ω_3 and ω_2 couple the flux on the intermediate state (curve B) to the doubly excited level (curve D).

Finally, Figs. 3(c–d) show that the blue sideband from EOM 2, ω_4, also provides a path from curve B to curve D, and explains why the vibrational structure cutoff extends further to the red in Fig. 2 from the normal (unsuppressed spectrum) frequency of $\simeq -1922$ MHz to $\simeq -3042$ MHz in the suppressed spectrum. In order to estimate the magnitude of the suppression effect, we have carried out model calculations at three levels of complexity: (1) time-dependent Monte Carlo wave function simulations [9] applied to wave-packet dynamics [10], including the effect of excited state decay, (2) standard quantum mechanical close coupling calculations without excited-state decay, and (3) semiclassical Landau-Zener estimates. These calculations will be described in detail in a separate publication [11], and we only summarize conclusions here.

In the present model, unit scattering flux, or quantum mechanical current $J(R_\infty) = 1$, starts at long range on the ground-state entrance channel, the one labeled 2 + 2 in Fig. 3. We calculate the current $J(R_p)$ reaching the point R_p, the Condon point where the probe-laser photon at frequency ω_p is absorbed. If ω_p is tuned to the blue of ω_3, so $R_p > R_S$, unit current reaches R_p and the probe excitation step is unattenuated [Fig. 3(d)]. But if ω_p is tuned to the red of ω_3, so $R_p < R_S$ [Fig. 3(c)], some current is deflected onto the repulsive state at R_s, less current reaches R_p, and PAI is reduced by the factor $1 - J(R_p)$. A Landau-Zener (LZ) model of the crossing predicts that

$$J(R_p) = e^{-A(R_s)}, \tag{1}$$

where

$$A(R_s) = 2\pi |V(R_s)|^2 / \hbar D(R_s) v(R_s). \tag{2}$$

Here $V(R_s)$ is the standard quasimolecular Rabi matrix element coupling the ground and excited molecular states [12],

$$V(R_s) = (2\pi I/3c)^{1/2} d(R_s). \tag{3}$$

In Eq. (3) I is laser power density, d is the transition dipole, and the $\sqrt{3}$ factor results from the root-mean-square average over all directions of the interatomic axis relative to the polarization vector of the light [13]. The velocity at the crossing is $v(R_s)$, and $D = d(C_3/R^3)/dR = 3C_3/R^4$ is the slope of the difference potential (the ground state is flat at long range). For our model we take typical parameters characteristic of Na to estimate the effect of the optical suppression: $C_3 = 10e^2a_0^2$, $d = 2.55ea_0$ (where e is the electron charge and a_0 the Bohr radius), and $\omega_S - \omega_1 = -2\pi(600\ \text{MHz})$ for the experimental case here.

Since the Condon point R_S lies very near the classical turning point of the repulsive potential, it is necessary to verify if the LZ expression remains valid for making estimates of suppression. The Monte Carlo simulations demonstrate that spontaneous decay during the dwell time near the turning point does not significantly modify the conclusions from using a quantum close-coupled model without decay, even when the field strength becomes large [11].

Figure 4 shows that there is excellent agreement between $J(R_p)$ calculated by quantum close coupling and by the LZ approximation, even at the Doppler cooling temperature 0.25 mK. Figure 4 also shows two experimental points for different intensities of the suppression laser. Evidently the simple two-state crossing model of Eq. (1) predicts reasonably well the observed magnitude of the suppression effect. Much more sophisticated calculations which include effects due to molecular hyperfine structure

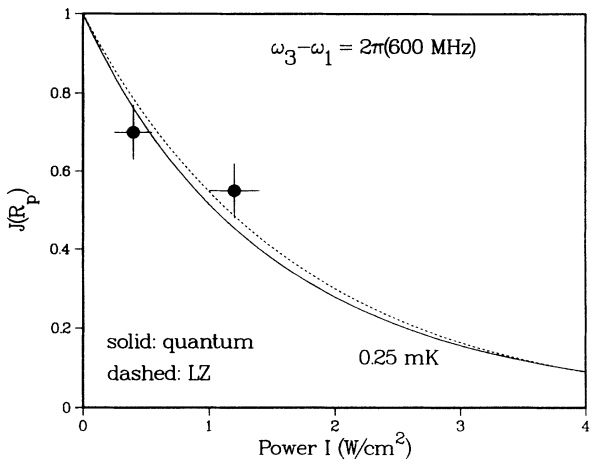

Fig. 4. Calculated flux J_p that penetrates to R_p on the ground-state A through the curve crossing at R_S. The curves compare quantum close coupled and Landau-Zener methods at collision energy E/k_B of 0.25 mK. Two experimental points of measured suppression vs intensity of ω_3 are also shown. The experimental MOT temperature is expected to be in this range.

and three-dimensional scattering are needed for a fully quantitative theory.

This paper has demonstrated that optical suppression of ultracold collisions is possible, and a very simple LZ model can confidently be used to predict the magnitude of the effect. The suppression of incoming scattering flux to small R, however, is not the only effect of the suppression laser. The LZ approximation shows that the fraction $2e^{-A}(1 - e^{-A})$ of collisions produces separating atoms in the excited repulsive state. Since energy conservation requires that these separating atoms share $\hbar\omega_3 - E(^2P_{3/2})$ in center of mass kinetic energy, these heated atoms may escape the confining potential. But if the intensity I is raised so that $A \gg 1$, the fraction of collisions that produce hot excited-state atoms becomes very small, and almost all colliding ground-state atoms would be repelled elastically upon reaching R_s.

Furthermore, any inelastic ground-state collisions due to interactions in the region with $R < R_s$ would be greatly suppressed. Although the effect of strong optical suppression on the performance of the trap itself remains to be investigated, it would be a most useful result if optical methods could be utilized to suppress undesirable collisions in order to increase trapped-atom densities, while enhancing ground-state elastic collisions. These concepts should be explored in the context of optical control of collisions as well as for achieving Bose-Einstein condensation of trapped alkali species [7].

We acknowledge the support of the University of São Paulo, the Conselho Nacional de Desenvolvimento Cientifico e Tecnolológico (CNPq), and the Fundacão de Amaparo a Pesquisa do Estado de São Paulo (FAPESP). J. W. acknowledges support from the National Science Foundation, the Army Research Office, and the National Institute of Standards and Technology. Acknowledgment is also made to the Donors of the Petroleum Research Fund, administered by the American Chemical Society, for partial support of this research. P. S. J. acknowledges support from the Office of Naval Research, and K.-A. S. acknowledges financial support from the Academy of Finland.

[1] For general reviews of ultracold collision dynamics see P. S. Julienne, A. M. Smith, and K. Burnett, Adv. At. Mol. Opt. Phys. **30**, 141 (1993); T. Walker and P. Feng, Adv. At. Mol. Opt. Phys. (to be published).

[2] C. D. Wallace, T. P. Dinneen, K.-Y. Tan, T. T. Grove, and P. L. Gould, Phys. Rev. Lett. **69**, 897 (1992); N. Ritchie, E. Abraham, Y. Xiao, C. Bradley, and R. Hulet, Laser Phys. (to be published).

[3] D. Sesko, T. Walker, C. Monroe, A. Gallagher, and C. Wieman, Phys. Rev. Lett. **63**, 961 (1989); P. Feng, D. Hoffmann, and T. Walker, Phys. Rev. A **47**, R3495 (1993).

[4] J. D. Miller, R. A. Cline, and D. J. Heinzen, Phys. Rev. Lett. **71**, 2204 (1993); L. Marcassa, V. Bagnato, Y. Wang, C. Tsao, J. Weiner, O. Dulieu, Y. B. Band, and P. S. Julienne, Phys. Rev. A **47**, R4563 (1993), and references cited therein.

[5] P. S. Julienne and R. Heather, Phys. Rev. Lett. **67**, 2135 (1991); P. Lett, P. Jessen, W. D. Phillips, S. Rolston, C. Westbrook, and P. Gould, Phys. Rev. Lett. **67**, 2139 (1991).

[6] V. Bagnato, L. Marcassa, C. Tsao, Y. Wang, and J. Weiner, Phys. Rev. Lett. **70**, 3225 (1993).

[7] E. Tiesinga, A. J. Moerdijk, B. J. Verhaar, and H. T. C. Stoof, Phys. Rev. A **46**, R1167 (1992).

[8] V. Bagnato, J. Weiner, P. S. Julienne, and C. J. Williams (unpublished).

[9] J. Dalibard, Y. Castin, and K. Mølmer, Phys. Rev. Lett. **68**, 580 (1992); Y. Castin, K. Mølmer, and J. Dalibard, J. Opt. Soc. Am. B **10**, 524 (1993).

[10] W. K. Lai, K.-A. Suominen, B. M. Garraway, and S. Stenholm, Phys. Rev. A **47**, 4779 (1993).

[11] K.-A. Suominen and P. S. Julienne (unpublished).

[12] P. S. Julienne, Phys. Rev. A **26**, 3299 (1982); F. H. Mies, in *Theoretical Chemistry: Advances and Perspectives*, edited by D. Henderson (Academic, New York, 1981), Vol. 6B, pp. 127–198.

[13] P. L. Devries and T. F. George, Mol. Phys. **36**, 151 (1978).

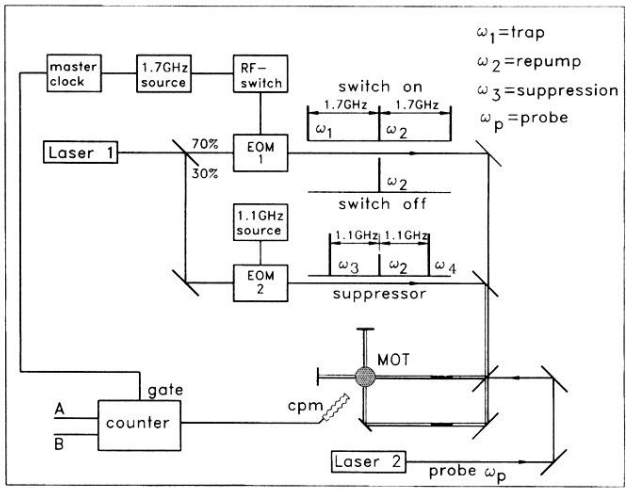

FIG. 1. Schematic diagram of the apparatus. The sidebands and carrier on the MOT laser are separated by 1712 MHz. The sidebands and carrier on the suppressor laser are separated by 1120 MHz.